University of Thi-Qar Journal of Science (UTJsci)
E-ISSN: 2709-0256, P-ISSN: 1991-8690, Vol. 12, No. 1, June. 2025

DFT Study in Strain Engineering $HfSe_2$ Nanosheets for Sensing SO_2, SOF_2, and SO_2F_2 Gases

Noora H. Ali[*1a] , Lafy F. Al-Badry[1b], and Ali Ben Ahmed[2, 3c]

[1]*Department of Physics, College of Science, University of Thi-Qar, Nassiriya, Thi-Qar 64001, Iraq*
[2]*University of Sfax, College of Science, Department of Physics, Sfax, Tunisia*
[3]*University of Sfax, Higher Institute of Biotechnology of Sfax, Department of Biomedical, Sfax, Tunisia*

[b]E-mail: lafi.faraj_ph@sci.utq.edu.iq, [c]E-mail: ali.benahmed@isbs.usf.tn

[a*]Corresponding author (Noora H. Ali): noorafofo33@sci.utq.edu.iq

Received: 2025-05-09, Revised: 2025-06-10, Accepted: 2025-06-16, Published: 2025-06-28

***Abstract*—Strain engineering is a technique of tuning a material's properties by modifying its mechanical or structural characteristics. Using first-principles calculations, the strain impact on the electronic structure of layered $HfSe_2$ nanosheets has been studied to examine the sensing capabilities of the layered $HfSe_2$ nanosheets to three SF_6 decomposition compounds (SO_2, SO_2F_2, and SOF_2). With biaxial strain, the band gap of the surfaces under discussion expands with tensile up to 1% and gradually decreases for strains between −1% and −5%. Additionally, our findings demonstrate that biaxial strains have a significant impact on the electronic characteristics, adsorption energy (E_{ad}), and desorption time of SO_2, SOF_2, and SO_2F_2 adsorbed $HfSe_2$ systems. The highest adsorption impact of SO_2, SOF_2, and SO_2F_2 on the bilayer of $HfSe_2$ occurred at a compressive strain of −5%, with the E_{ad} determined as −1.34, −1.27, and −1.31 eV, respectively. These external factors are widely preferred and offer a workable solution for tunable $HfSe_2$-based gas sensors and electrical devices under biaxial compressive strain.**

Keywords*— *Strain engineering, Monolayer $HfSe_2$, Bilayer $HfSe_2$, SF_6 gas, Gas sensor.

I. INTRODUCTION

To ensure the electricity system's safe operation, SF_6 gas, which has exceptional insulating strength and arc-extinction properties, is frequently used in extra-high voltage equipment [1-2]. However, the inevitably occurring insulating flaws, such as partial discharge and partial overheating during extended use of power equipment, would break down SF_6 over time into several ionized F atoms and low-fluorine sulfides [3]. While these low-fluorine sulfides can often recombine with F atoms to produce SF_6 once more, in the presence of trace amounts of water and oxygen, the sulfides would continue to react with the impure elements to generate a variety of stable gas species, including H_2S, SO_2, SOF_2, and SO_2F_2 [4-5]. These SF_6 decomposition components are dangerous to the environment and human health, speeding up facility corrosion and raising the likelihood of system paralysis [6]. Therefore, operational detection of these typical SF_6 breakdown components is crucial. In this regard, it has been determined that the detection of SF_6 decomposed species, particularly SO_2, SOF_2, and SO_2F_2, is a practical and efficient method for assessing the operational state of SF_6 insulating devices, which is also significant to ensure the smooth operation of the entire power system [7-8]. Therefore, monitoring the decomposition components, taking precautions promptly, and ensuring the safe operation of power equipment would be possible and practical using gas sensors and adsorbents with ultrahigh-sensitivity and selective qualities [4].

As a result, a wide range of two-dimensional (2D) layered nanosheets, including graphene [9], boron-phosphorus [10], aluminium nitrate [11], aluminum phosphate [12], and silicone [13]. They draw considerable interest due to their distinctive architectures and exceptional characteristics. Due to the structural stability, chemical inertness, and physical properties, the 2D MX_2 family (transition metal dichalcogenides (TMDs); MX_2: M = transition metals (TM); X = chalcogen) has lately demonstrated tremendous potential as gas sensors [14-16]. TMD materials for gas sensing have received a lot of attention, including MoS_2 [17, 18], $MoSe_2$ [19], PdS_2 [16], $PtTe_2$ [20] , and wS_2 [21]. For example, Li et al. [22] examine and evaluate the outcomes of MoS_2-based gas sensors and concluding that 2D MoS_2 may be suitable for creating high-performance ambient-temperature gas sensors. While other TMD types, such as ZrX_2 and HfX_2 (X = Se, S, and Te), have received less research. $HfSe_2$ nanosheet has been predicted theoretically to have a small band gap and strong carrier mobility [23]. Numerous scientific experiments have successfully produced the monolayer [24], which suggests that it might be used as a material for gas sensors.

A popular technique for enhancing the nano-system's chemical reaction and catalytic behaviour, and hence enhancing the adsorption and sensing capabilities of the nano-materials, is surface-doping by TM [25-29]. Extensive research on TMDs as SF_6 decomposition sensors, such as MoS_2[30, 31] and $MoTe_2$ [32]. sensors, has been done during the last few decades. According to the investigations, Ga-MoS_2 might be an excellent gas-sensing material for SO_2 and

https://doi.org/10.32792/utq/utjsci/v12i1.1393

SO_2F_2; however, because of its limited adsorption, it was not a good fit for SOF_2 sensing [31]. On the other hand, using first-principles calculations, Cui Hao et al. [33-34] investigated the adsorption behaviour of pristine, and Pt-doped $HfSe_2$ monolayers to some hazardous gases (SOF_2, SO_2, and NO_2). It is discovered that the Pt-doped $HfSe_2$ monolayer exhibits better behavior for SO_2. Rh-doped $HfSe_2$'s adsorption nature and behavior were investigated by Wang et al. [35], and their findings indicate that SO_2 and the monolayer interact more strongly than SO_2F_2. Additionally, our group [36] reported that monolayer $HfSe_2$ doped with a nickel cluster could distinguish SF_6 decomposition gases, also exhibiting excellent sensitivity and regulated gas release/ storage. Besides, nano-sensors improved sensing capabilities can enable their use in harsher environments with a strong sensitivity toward gaseous species [37-38], which is urgently needed in material science and engineering [39- 40]. For adsorption systems, control over charge transfer and electronic structures would impact both sensing performance and adsorption capabilities [41- 42].

Applying external strain to the adsorption system is one efficient method for tuning the electronic characteristics [43- 44]. For example, Guzman and Strachen [45] forecast significant changes in bandgap for several monolayer TMDs with biaxial strain ranging from −5% to 5%. According to Li et al.'s research [46] The Ru-$PtSe_2$ monolayer has a tunable sensing response for gas detection with modulated strains, as evidenced by its increased sensitivity to C_2H_2 detection by manipulating biaxial strains. The SnS_2 sheets also demonstrate how biaxial strains can significantly alter the adsorption energy, electronic characteristics, and charge transfer of systems with adsorbed nitrogen dioxide [47]. According to Ni et al.'s findings, the adsorption capabilities of an Ag-doped WSe_2 monolayer declined as the biaxial strain increased [48].

In this study, we design models for SO_2, SOF_2, and SO_2F_2 adsorption on pure monolayer and bilayer $HfSe_2$ nanosheets to compute the adsorption behaviors, and investigate their potential as gas sensors under applying biaxial strain. Our research may pave the path for using $HfSe_2$ to identify SF_6 decompositions in challenging application environments, including the interior of gas-insulated switchgear (GIS) equipment.

II. Computational Methods

All computations on $HfSe_2$ nanosheets are performed with DFT via the DMol3 package[49] by using the material studio program, and considering the impact of spin polarization, peripheral electrons for Hf (Se) are produced in a $5d^2$ $6s^2$ ($4s^24p^4$) configuration (32 Se atoms and 16 Hf atoms). The generalized approximation gradient (GGA) and Perdew-Burke-Ernzerhof (PBE) are utilized to handle the exchange-related energy [50], where the PBE functional is very popular because it is a non-empirical functional with reasonable accuracy over a wide range of systems. While PBE is typically not the most accurate GGA functional (especially for band gap) for a given system, it usually is not too far off either [51]. In addition, GGA struggles to adequately describe long-range effects like vdWs [52]. To investigate the reactions between $HfSe_2$ sheets and gas molecules, the long-range dispersion-corrected developed by Tkatchenko-Scheffler (TS) has been utilized. TS offers empirical parameters for the elements' surface ($HfSe_2$ sheets), whereas Grimme don't offered it [53]. The basis set was specificed by double numerical plus polarization (DNP). We used the appropriate number of Monkhorst-Pack k-point grids, 7 × 7 × 1, and mesh smearing of 0.005 Ha for the geometry optimization and the electronic attribute computations. All structural models were completely relaxed until the maximum force and the tolerance energy were less than 0.002 Ha/Å and 10^{-5} eV, respectively. In addition, the self-consistent field (SCF) tolerance was set to 10^{-6} Ha [54]. A supercell was large enough for 4 × 4 × 1 $HfSe_2$ sheets [33, 35, 55]. To avoid erroneous interactions between the periodic pictures, a 20 vacuum was placed between them along the z-axis. The adsorption energy (E_{ad}) is defined as the energy required to adsorb a certain amount of gas onto a $HfSe_2$ sheet [56], which is quantitatively described as follows:

$$E_{ad} = E_{surf/gas} - E_{surf} - E_{gas} \quad (1)$$

where $E_{surf/gas}$, E_{surf} and E_{gas} are the total energy of gas adsorption systems, isolated surfaces, and the separated gas molecules, respectively. Here, the stronger the adsorption, the more negative the E_{ads}. Hirshfeld population analysis can be used to examine the charge transfer (Q_t) of the gas molecules adsorbed on layered $HfSe_2$ sheets [56]. Q_t denotes the quantity of charge transfer between substrates and the gas molecules.

$$Q_t = Q_{tiso} - Q_{tads} \quad (2)$$

where Q_{tiso} stands for the isolated gas molecules and Q_{tads} for the total charges carried of the adsorbed gas.

III. Results and Discussion

A. The Geometric and Electronic Properties

Fig. 1 (a, b) shows the top and side views of the optimized structures of the $HfSe_2$ monolayer and bilayer. The P3-m1 space group (No. 164) is home to the tetragonal symmetry found in $HfSe_2$ sheets. Se, Hf, and Se atoms are stacked one on top of the other to form their structure. The internal coordinates are (0, 0, 0) and (1/3, 2/3, 0.227) for Hf and Se, respectively. The researched material's optimal lattice parameters are a = b = 3.75 Å, which agree with the theoretical conclusions that have already been established [34, 36]. Interatomic distance Se-Hf is 2.69 Å at equilibrium, and the lattice angles of α= β=90.00° and γ = 120.00°. In our study, AA (eclipsed with Se (Hf) over Se (Hf)) is the order in which the $HfSe_2$ bilayer was stacked; the interlayer gap between Se and Se is 6.084 Å. The band structure (BS) and density of states (DOS) of the unstrained $HfSe_2$ monolayer and bilayer are shown in Fig. 1(c, d), respectively. Given that the conduction band (CB) minimum is identified at the M point and the valence band (VB) maximum is discovered at point Γ close to the Fermi level, the profile of the derived BS suggests that the investigated sheets are an indirect semiconductor. The monolayer and bilayer systems' resulting band gaps are 0.477 eV (which agrees with the previously reported value [34-54]) and 0.429 eV, respectively. As observed in the figure, the extent of the energies is limited from −3 eV to 3 eV (−2 eV to 2 eV) for monolayer (bilayer), the VB is dominated mainly by Se atoms, with a modest contribution from Hf atoms, while both atoms contribute to the CB. The response of Se and Hf atoms in the $HfSe_2$

monolayer and bilayer is reasonable for the hybridization among Se 4p and Hf 5d states, and the hybridization occurs significantly farther from the Fermi level.

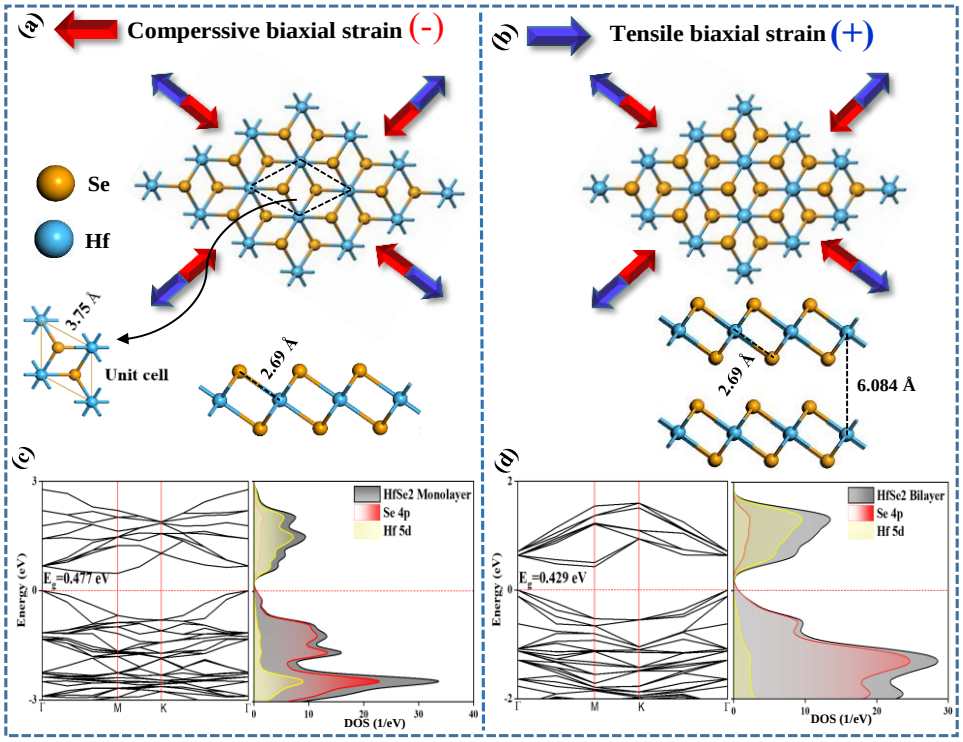

Fig. 1: Geometric structure, BS, and DOS of (a,c) monolayer $HfSe_2$ and (b,d) bilayer $HfSe_2$.

B. Adsorption Unstrained Systems

To determine the most favorable adsorption configuration, the three gas molecules were placed molecules at three possible sites above the pristine $HfSe_2$ monolayer and bilayer positions classified as: 1-the top Se atom of the downer layer, i.e. gas molecules above the center of hexagonal ring of $HfSe_2$, 2- the top of Hf atom, 3- the top of Se of the upper layer. The three aim gases were adsorbed using the best model of $HfSe_2$ sheets. The adsorption features of $HfSe_2$ sheets were investigated in light of the adsorption parameters (represented by E_{ad}, Q_t, and distance between Se and S atoms), which are listed in Table 1. The ideal adsorption models of three gases (SO_2, SOF_2, and SO_2F_2) on the $HfSe_2$ sheets are shown in Fig. 2. All systems have long adsorption lengths and low Q_t value, indicating insensitive physisorption, as indicated by the values in Table 1.

Table 1. Adsorption characteristics of SO_2, SOF_2, and SO_2F_2 gases on $HfSe_2$ sheets

Structure	Gas molecules	Figure	E_{ad} (eV)	Q_t Hirshfeld (e)	D (Å) S-Se
$HfSe_2$ monolayer	SO_2	Fig. 2(a1)	-0.32	-0.076	3.194
	SOF_2	Fig. 2(b1)	-0.247	-0.0008	3.692
	SO_2F_2	Fig. 2(c1)	-0.279	-0.0031	3.866
$HfSe_2$ bilayer	SO_2	Fig. 2(a2)	-0.294	-0.0785	3.173
	SOF_2	Fig. 2(b2)	-0.214	-0.0015	3.687
	SO_2F_2	Fig. 2(c2)	-0.255	-0.0047	4.03

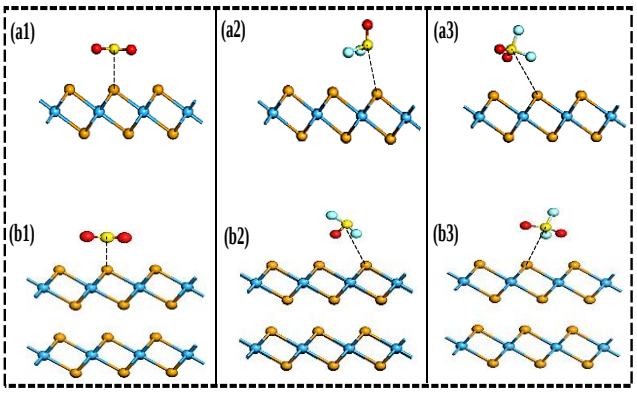

Fig.2: Side view of SO_2, SOF_2 and SO_2F_2 adsorption systems, above (a1-a3) monolayer and (b1-b2) bilayer $HfSe_2$.

C. Electronic Properties under Strain

Fig. 1 shows the schematic diagrams of applying tensile and compressive biaxial strain on $HfSe_2$ sheets before gas adsorption, where positive and negative values represent tensile and compressive strain, respectively. Strain engineering is one of the most efficient ways to control the electronic characteristics of semiconductors. It is widely known that altering the electronic characteristics of semiconductor materials is crucial for gas sensors. Biaxial strain is more effective than uniaxial strain in adjusting the adsorption properties [57]. Based on the literature that predicted large band gap changes for several monolayer TMDs with biaxial strain ranging from −5% to 1%. The monolayer shows a transition from semiconductor to metal at −5% with surface stability [45]. Therefore, we examined the

electronic characteristics of the monolayer and bilayer of $HfSe_2$ while subjected to an external biaxial strain. The lattice constants of the strained and unstrained systems, a and a_0, respectively, are used to calculate the biaxial strain [56]. which is defined as $\varepsilon = (a - a_0)/a_0 \times 100\%$. Only the atomic position can relax for the strained system. Here, strains between −5% and 1% with a step of 2% are taken into consideration; the strain is set with lattice constants of 3.563, 3.637, 3.713, and 3.788 Å, respectively. Three negative/positive strain values correspond to compressive/tensile strains. Analyzing their BSs and DOS prior to gas adsorption is vital to comprehend their adsorption properties under biaxial strain with values −5%, −3%, −1%, and 1%, see Figs. 3 and 4 of monolayer and bilayer, respectively. We discovered that the monolayer and the bilayer have an indirect BG at zero strain and that the gap (decreases) increases at (compressive) tensile uniform strain. The band gaps of the monolayer and bilayer remain indirect for all strain values considered. In the case of a bilayer, the maximum VB changes from Γ to M because the state at M gains energy under tensile strain, although the corresponding eigenvalue at Γ does not significantly change. We can observe that the minimum CB and the maximum VB were always found at the M and Γ point, respectively. Hence, the lack of contrast in maximum VB and the minimum CB governed the non-switch from indirect to direct BG. Keep in mind that negative strain values represent compressive strain. The impact of mechanical distortions on the electronic structure is primarily discernible at the M-K path, where the bottom of the CB is drastically decreased relative to the equilibrium status. The top of VB at the Γ spot travels upward concurrently. Because of the alteration in bond lengths, this behavior is understandable makes sense because the orbital overlap between the Hf and Se atoms reduces. The electron conductivity in semiconducting TMD nanosheets can be increased or decreased due to changes in the electronic architecture caused by mechanical deformations. The BG is decreased due to the 2D-compressive strain, and the electron conductivity at the Fermi level is noticeably increased. Since the BGs of the $HfSe_2$ monolayer (bilayer) vanish at about −5% (−3%) strain, the transport paths are open, enabling electrical conductivity. This can be described by the Brillouin zone deformation, where the applied strain evenly alters the primitive cell, bands penetrate the Fermi level, and as a result, a monolayer's (bilayer's) character transforms from semiconducting to metallic. Additionally, it is intriguing to observe that the bilayer's interlayer spacing marginally increases with compressive strain and reduces with tensile strain, as seen in Fig. 5.

D. Enhancement of sensing features under strain

Adsorption systems under biaxial strain ranging from −5% ~ 1% are monitored in order to assess the impact of applied strain on the potential for adsorption and sensing performance of $HfSe_2$ sheets towards SO_2, SOF_2, and SO_2F_2. The E_{ads} and Q_t with various biaxial strains are depicted in Fig. 6 and 7. The findings demonstrate that applying biaxial strain significantly affects the E_{ad} for all systems, increasing E_{ads} as tensile strain increases. However, as the compressive strain is increased, the adsorption diminishes. In both systems, a better response performance for the sensing material to the target gas is generally correlated with lower E_{ads}. The SO_2F_2 molecule has the same behavior in both systems, but the bilayer exhibits a more considerable sensitivity to the SO_2 and SOF_2 molecules under compressive strains of up to −5% as the E_{ad} gets more negative (−1.34 and −1.27 eV, respectively).

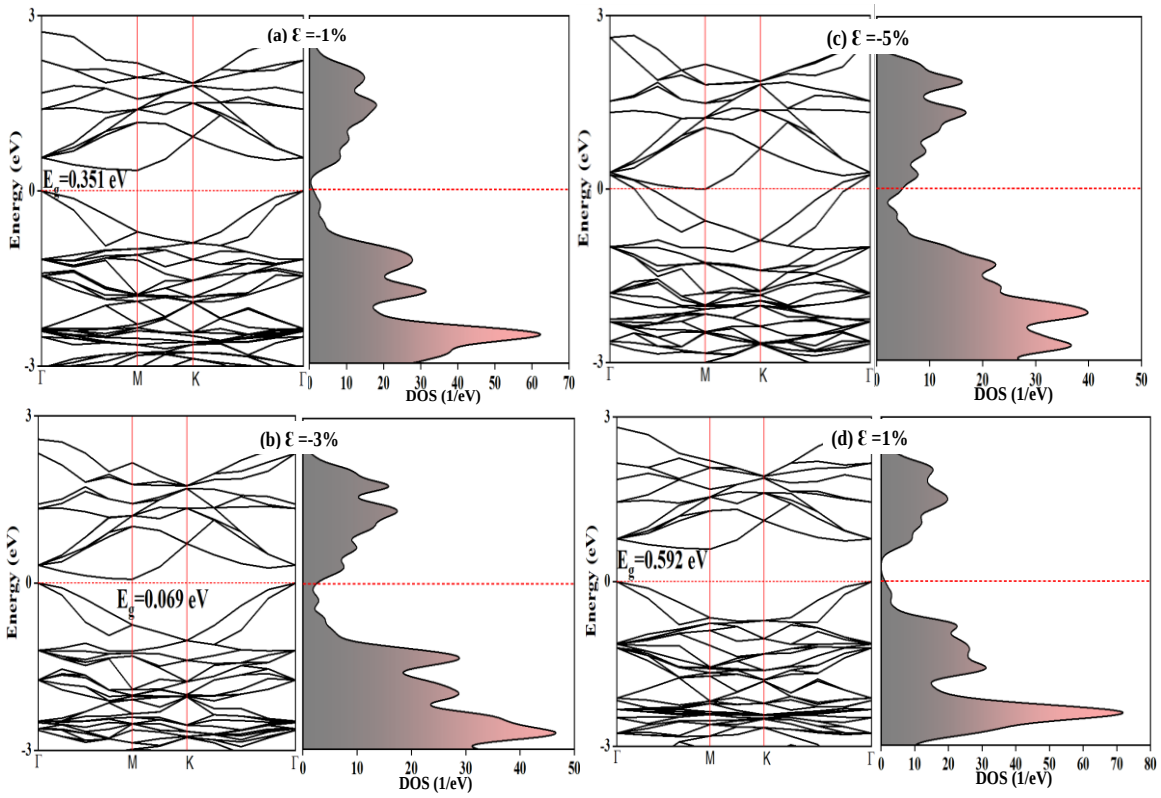

Fig. 3: BGs and DOS for monolayer $HfSe_2$ in the presence of biaxial strain, represented by the dashed red line at the Fermi level (tuning to zero).

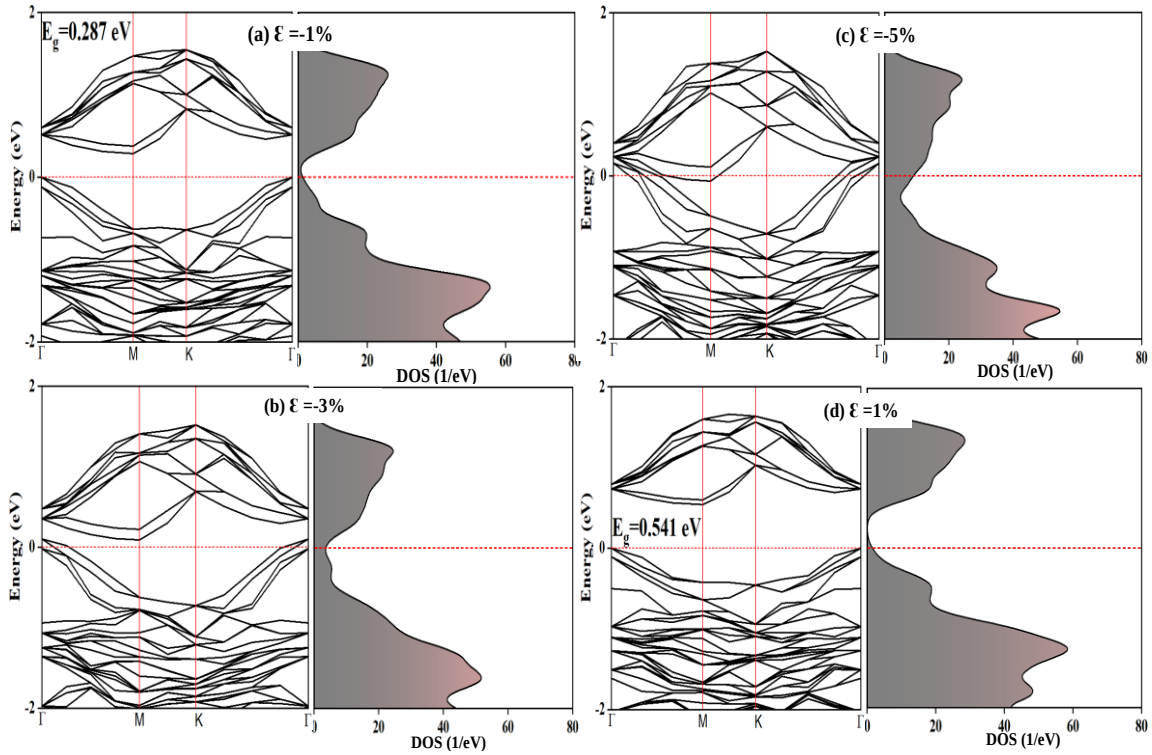

Fig. 4: BGs and DOS for bilayer $HfSe_2$ in the presence of biaxial strain represented by the dashed red line at the Fermi level (tuning to zero).

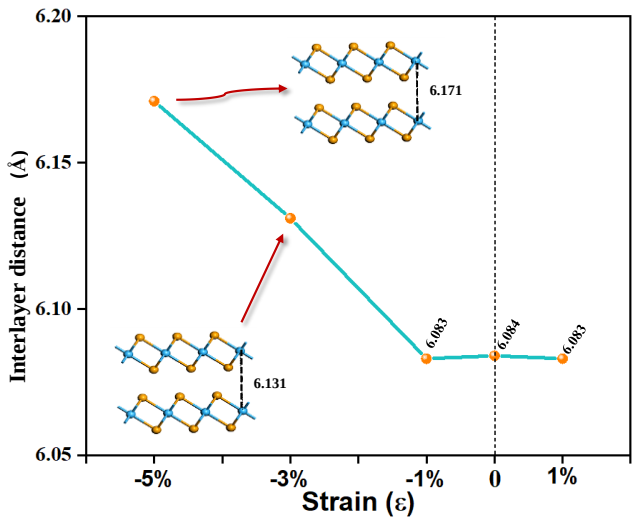

Fig. 5: Interlayer distance for bilayer $HfSe_2$ as a function of biaxial strain applied, distance in Å.

On the other hand, when the tensile strain reaches 1%, it is expected that the E_{ad} of the $HfSe_2$ bilayer system will be −0.0803, + 0.0038, and −0.0403 eV for SO_2, SOF_2, and SO_2F_2, respectively. This indicates that the adsorption mechanism is weak or non-existent for bilayer systems with a 1% tensile strain. Due to the bilayer system's instability at 1% tensile biaxial strain, the gas molecules are independent of the surface. In other words, the system had some difficulty in adsorption of these gases[31].

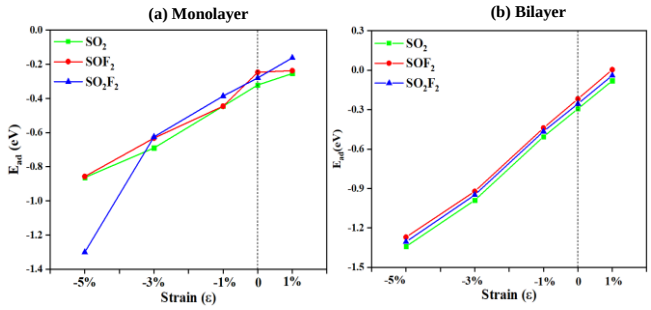

Fig. 6: Variation of the E_{ads} for SO_2, SOF_2, and SO_2F_2 adsorbed on (a) monolayer $HfSe_2$ and (b) bilayer $HfSe_2$ as a function of biaxial strain.

In related adsorption systems, the Q_t exhibits a similar tendency as a function of biaxial strain. After adjusting the biaxial strain from −5% to 1%, −0.080 and −0.0787 electrons were transferred by the $HfSe_2$ monolayer and bilayer from the SO_2 molecule at −5% strain, respectively. Upon examining different systems, it is notable that SO_2-$HfSe_2$ adsorption systems have the highest Q_t sensitivity. After applying the biaxial strain, there was clear change in the Q_t of the SO_2-$HfSe_2$ system from -0.08 to −0.0903e for biaxial strain from −5% to 1%, respectively. This result is considered important compared with the charge transfer values in Ref. [58]. where Q_t ranges from 0.008 to 0.019e for biaxial strain from −4% to 1%, respectively.

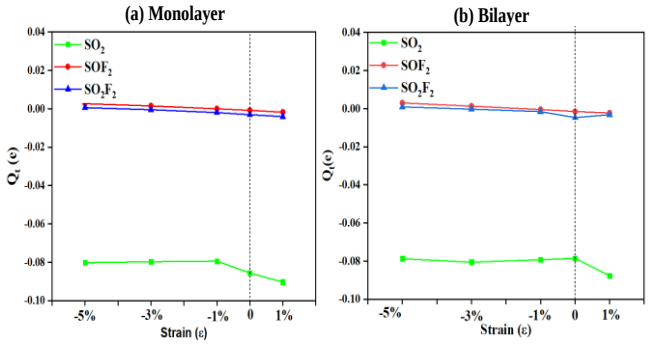

Fig. 7: Variation of the Q_t for SO_2, SOF_2, and SO_2F_2 adsorbed on (a) monolayer $HfSe_2$ and (b) bilayer $HfSe_2$ as a function of biaxial strain.

In contrast, the SOF_2 and SO_2F_2 adsorption systems (related to low charge transfer) do not experience any substantial Q_t following the addition of external strain. According to Hirshfeld analysis, for SOF_2-adsorbed monolayer and bilayer $HfSe_2$ nanosheet at −5% strain, there are 0.0027 e and 0.003 e moving from the substrate to SOF_2 molecule, respectively. The SO_2F_2 adsorption systems behave similarly to SOF_2 systems in Q_t as well. Even if these two gases continue to have the electron donor feature, we might see a change in the charge transport path in the two systems when the applied strain drops below −3%.

In Fig. 8(a and b), we present the relationship between strain and the adsorption distance (d) of $HfSe_2$ systems. Both systems show slight decrease in the S-Se adsorption distance for the gas molecules with the increase of compression strain (from 0 to −5%), where the absolute value of E_{ad} increases from 0.32 ~ 0.86 eV (0.29 ~ 1.34 eV), 0.247~0.85 (0.22 ~ 1.27 eV)and 0.279~1.3 (0.255 ~ 1.31 eV) for the adsorption SO_2, SOF_2, and SO_2F_2 on $HfSe_2$ monolayer (bilayer), and a decreasing tendency in the d-curve indicates stronger binding at a reduced adsorption distance. Except for the adsorption of SO_2F_2 gas on the bilayer, we can see that the distance increases and then decreases at −5% strain.

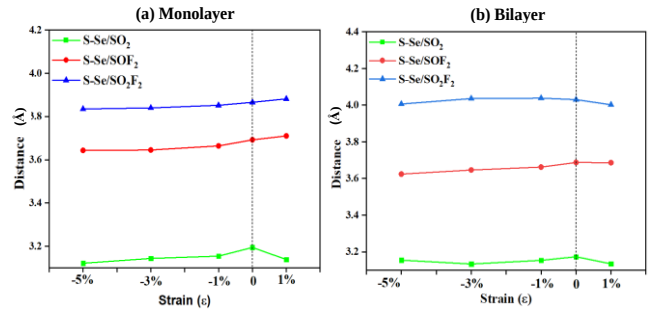

Fig. 8: Variation of the adsorption distance for SO_2, SOF_2, and SO_2F_2 adsorbed on (a) $HfSe_2$ monolayer and (b) $HfSe_2$ bilayer as a function of biaxial strain.

Initially, we computed the BSs of the studied structures under biaxial strain. The variance in BG with strain is illustrated in Fig. 3 and 4. Generally, compressive strain causes a decrease in the BG of all studied systems. The effect of tensile was slightly different, the BG rising as the biaxial strain increased. The BGs of the gas-adsorbed systems exhibit a linear relationship in Fig. 9 (a and b), slightly narrower when subjected to compressive strain and broader when tensile strains are applied. In other words, despite both systems being strain-sensitive and giving diverse sensing responses, the $HfSe_2$ bilayer has greater sensitivity upon gas detection with the modification of biaxial stresses. Adding biaxial strain has less impact the unadsorbed $HfSe_2$ monolayer, which retains its semiconductor nature except for a compressive strain of up to −5% when the monolayer turns metallic.

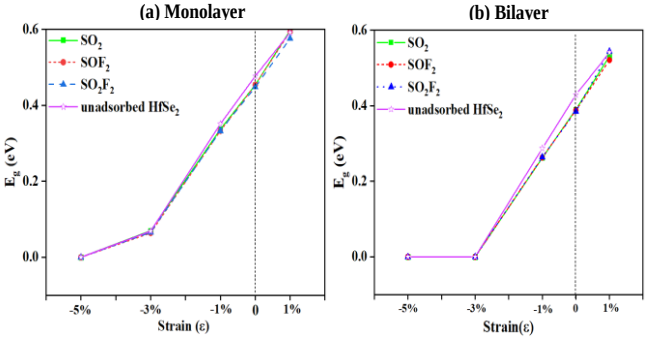

Fig. 9: Variation of the BS for SO_2, SOF_2, and SO_2F_2 adsorbed on (a) $HfSe_2$ monolayer and (b) $HfSe_2$ bilayer as a function of biaxial strain.

E. Recovery Time

Recovery time (τ), which indicates whether the material is acceptable for practice application reality or not, is another essential merit quality. According to the Arrhenius formula, the relationship between τ and desorption barrier E_a (is equal to E_{ad}) is estimated as follows:

$$\tau = \nu_0^{-1} e^{-E_a/k_B T} \quad (3)$$

Here, ν_0 is the operational frequency, which is taken as 10^{12}Hz, k_B is the Boltzmann constant, and T is the operational temperature (300 K) [59]. The τ is defined by the time it takes the target material ($HfSe_2$ sheets) to reestablish its pristine properties or condition once the gas molecule is removed, determining how long the $HfSe_2$ sheets can be reused. Fig. 10(a, b) shows the weighted τ as a function of biaxial strain. According to the calculations shown in Fig. 10, the adsorption time of gas molecules of all systems gets faster (or instantaneously) under the tensile strains and increases linearly under the compressive strains.

For the adsorption on the $HfSe_2$ monolayer, SO_2F_2 has the largest E_{ad} under the compressive strain of up −5%, which means that the reaction between SO_2F_2 and the $HfSe_2$ monolayer is the most powerful. However, the desorption barrier is higher with a high E_{ad}. Since the SO_2F_2 molecule has a much higher estimate of the τ (9.8×10^9 s) than the other two gas molecules, it has the lowest absorption rate. The other two gases have a higher absorption rate due to a lower absorption barrier, and the corresponding τ (6.6 and 5.15 min for SO_2 and SOF_2 gases, respectively) is also shorter .

For the desorption from the $HfSe_2$ bilayer, all the E_{ads} of these three gas molecules are more significant than those on the $HfSe_2$ monolayer under the compressive strain. They have higher desorption barriers as a result, which results in slower absorption rates and longer τ. Applying compressive strain significantly lengthens the τ. $HfSe_2$ sheets have a

more remarkable detection ability when the target gas binds to the surface for a long time. On the other hand, biaxial tensile strain would result in a noticeably reduced τ for each system under consideration, indicating that biaxial tensile strain might be used to desorb gas quickly. For instance, the τ of the gases/$HfSe_2$ bilayer adsorption system is drastically reduced when the external strain of −5% changes to that of 1%. As a result, the analysis of τ shows that controlling external factors is necessary to regulate the adsorption-absorption process. Due to the combination of the sheets' selectivity of $HfSe_2$, greater $E_{ad,}$ and the high τ, the bilayer is more effective than the monolayer in detecting SF_6 breakdown products.

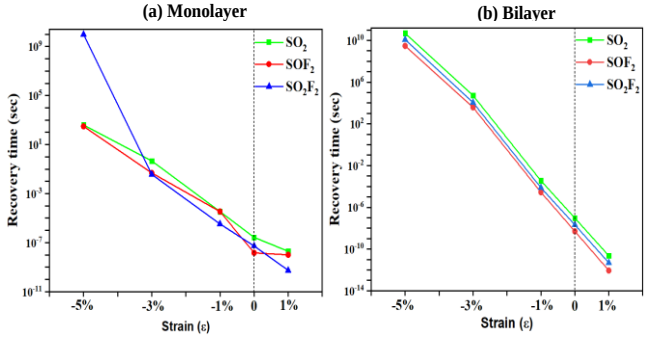

Fig. 10: Variation of the recovery time for SO_2, SOF_2, and SO_2F_2 adsorbed on (a) $HfSe_2$ monolayer and (b) $HfSe_2$ bilayer as a function of biaxial strain.

IV. CONCLUSIONS

In brief, the sensor mechanism of layered $HfSe_2$ towards three common gases resulting from SF_6 decomposition is investigated using first-principles calculations. The geometrical stability and electronic characteristics of SO_2, SOF_2, and SO_2F_2 on the $HfSe_2$ monolayer and bilayer are monitored under biaxial strain engineering. According to the electronic systems study, biaxial strain could be used to successfully control the electrical conductivities of the surfaces under consideration, while the adsorption of gas molecules does not generate noticeable changes in the electronic properties of the surfaces. However, the E_{ad} of all systems increases after applying compressive strain, while the tensile biaxial strain decreases the E_{ad}. The findings demonstrate that the E_{ads} of SO_2 and SOF_2 molecules on a monolayer (−0.86 and −0.85 eV, respectively) are lower than that for SO_2F_2 adsorption (−1.30 eV) system at −5% strain, indicating that the application of compressive strain increased the $HfSe_2$ monolayer's sensitivity to SO_2F_2. In addition, the bilayer shows high adsorption energy towards all gases in the following order: SO_2(−1.34)> SO_2F_2(−1.31)>SOF_2(−1.27). Moreover, the computed recovery times for each system showed that tensile strain assisted–absorption, whereas compressive strain enhanced gas adsorption. The study suggested that $HfSe_2$ nanosheets are a promising bidirectional sensing material for SF_6 decomposition detection, which can be manipulated by applying biaxial strain.

CONFLICT OF INTEREST

Authors declare that they have no conflict of interest.

REFERENCES

[1] H. Cui, T. Liu, Y. Zhang, and X. Zhang, "Ru-InN monolayer as a gas scavenger to guard the operation status of SF 6 insulation devices: A first-principles theory," *IEEE Sensors Journal*, vol. 19, no. 13, pp. 5249-5255, 2019.

[2] A. Dong and M. Liu, "A DFT study on the adsorption properties of Ti3C2O2 MXene towards SF6 decomposition gases," *Surface Science*, vol. 734, p. 122317, 2023.

[3] X. Zhang, L. Yu, Y. Gui, and W. Hu, "First-principles study of SF6 decomposed gas adsorbed on Au-decorated graphene," *Applied Surface Science*, vol. 367, pp. 259-269, 2016.

[4] Y. Gui, J. Shi, P. Yang, T. Li, C. Tang, and L. Xu, "Platinum modified MoS2 monolayer for adsorption and gas sensing of SF6 decomposition products: A DFT study," *High Voltage*, vol. 5, no. 4, pp. 454-462, 2020.

[5] F. Zeng, J. Tang, Y. Xie, Q. Zhou, and C. Zhang, "Experimence study of trace water and oxygen impact on SF 6 decomposition characteristics under partial discharge," *Journal of Electrical Engineering & Technology*, vol. 10, no. 4, pp. 1786-1795, 2015.

[6] A.-J. Yang *et al.*, "Phosphorene: A promising candidate for highly sensitive and selective SF 6 decomposition gas sensors," *IEEE Electron Device Letters*, vol. 38, no. 7, pp. 963-966, 2017.

[7] X. Zhang, L. Yu, J. Tie, and X. Dong, "Gas sensitivity and sensing mechanism studies on Au-doped TiO2 nanotube arrays for detecting SF6 decomposed components," *Sensors*, vol. 14, no. 10, pp. 19517-19532, 2014.

[8] H. Zhao *et al.*, "Understanding competitive adsorption of SF6 and its decomposed components on α-Fe2O3," *Surface Science*, vol. 723, p. 122128, 2022.

[9] Z. Chen, J. Wang, and Y. Wang, "Strategies for the performance enhancement of graphene-based gas sensors: A review," *Talanta*, vol. 235, p. 122745, 2021.

[10] S. Thomas, V. Kumar, D. R. Roy, and M. A. Zaeem, "Two-dimensional boron–phosphorus monolayer for reversible NO2 gas sensing," *ACS Applied Nano Materials*, vol. 3, no. 10, pp. 10073-10081, 2020.

[11] W. Abdul-Hussein, F. H. Hanoon, and L. F. Al-Badry, "Control the electronic and optical properties of AlN nanosheet by the electric field," *Results in Optics*, vol. 11, p. 100423, 2023.

[12] W. Abdul-Hussein, F. H. Hanoon, and L. F. Al-Badry, "Designing sub-5 nm monolayer AlP MOSFETs," *Micro and Nanostructures*, vol. 176, p. 207524, 2023.

[13] G. K. Walia, D. K. K. Randhawa, and K. S. Malhi, "Rise of silicene and its applications in gas sensing," *Journal of Molecular Modeling*, vol. 27, pp. 1-11, 2021.

[14] F. Opoku and P. P. Govender, "Highly selective and sensitive detection of formaldehyde by β12-

borophene/SnO2 heterostructures: the role of an external electric field and in-plain biaxial strain," *The Journal of Physical Chemistry A*, vol. 124, no. 11, pp. 2288-2300, 2020.

[15] C. Niu *et al.*, "Tunable adsorption behavior of small molecule on GeP monolayer by applied strain and electric field," *Applied Surface Science*, vol. 520, p. 146257, 2020.

[16] Y. Ma, X. Gong, F. Xiao, Y. Liu, and X. Ming, "First-Principles Study on the Selective Detection of Toxic Gases by 2D Monolayer PdS2: Insight into Charge Transfer Dynamics and Alignment of Frontier Molecular Orbitals," *ACS Applied Nano Materials*, vol. 6, no. 13, pp. 12470-12478, 2023.

[17] H. Ye *et al.*, "SnSe monolayer: A promising candidate of SO2 sensor with high adsorption quantity," *Applied Surface Science*, vol. 484, pp. 33-38, 2019.

[18] L. Liu *et al.*, "High selective gas detection for small molecules based on germanium selenide monolayer," *Applied Surface Science*, vol. 433, pp. 575-581, 2018.

[19] C. Gao *et al.*, "A DFT study of In doped Tl2O: a superior NO2 gas sensor with selective adsorption and distinct optical response," *Applied Surface Science*, vol. 494, pp. 162-169, 2019.

[20] N. H. Ali and L. F. Al-Badry, "Mo-PtTe2 monolayer as a promising biosensor for prediagnosis of lung cancer: A DFT study," *Computational and Theoretical Chemistry*, vol. 1230, p. 114379, 2023.

[21] H. Cui, X. Zhang, G. Zhang, and J. Tang, "Pd-doped MoS2 monolayer: A promising candidate for DGA in transformer oil based on DFT method," *Applied Surface Science*, vol. 470, pp. 1035-1042, 2019.

[22] B. Li, Q. Zhou, R. Peng, Y. Liao, and W. Zeng, "Adsorption of SF6 decomposition gases (H2S, SO2, SOF2 and SO2F2) on Sc-doped MoS2 surface: A DFT study," *Applied Surface Science*, vol. 549, p. 149271, 2021.

[23] M. Salavati, "Electronic and mechanical responses of two-dimensional HfS2, HfSe2, ZrS2, and ZrSe2 from first-principles," *Frontiers of Structural and Civil Engineering*, vol. 13, no. 2, pp. 486-494, 2019.

[24] R. Kumar, N. Goel, M. Hojamberdiev, and M. Kumar, "Transition metal dichalcogenides-based flexible gas sensors," *Sensors and Actuators A: Physical*, vol. 303, p. 111875, 2020.

[25] Y. Fan, J. Zhang, Y. Qiu, J. Zhu, Y. Zhang, and G. Hu, "A DFT study of transition metal (Fe, Co, Ni, Cu, Ag, Au, Rh, Pd, Pt and Ir)-embedded monolayer MoS2 for gas adsorption," *Computational Materials Science*, vol. 138, pp. 255-266, 2017.

[26] D. Ma *et al.*, "The adsorption of CO and NO on the MoS2 monolayer doped with Au, Pt, Pd, or Ni: A first-principles study," *Applied Surface Science*, vol. 383, pp. 98-105, 2016.

[27] H. C. Sari *et al.*, "Computational molecular design to assist modification of single–walled carbon nanotubes with B, N, Al, Si, P, and S dopant atoms for Cl2 gas sensor application," *Surface Science*, vol. 731, p. 122264, 2023.

[28] R. Zhang, Z. Liu, D. Holiharimanana, and H. Sun, "Renewable Adsorption/Desorption of Sarin on TM-Doped CNTs: First Principle Calculations," *Surface Science*, vol. 736, p. 122338, 2023.

[29] F. Thamer, A. S. Alwan, and A. B. Ahmed, "Studying the electronic characteristics and physisorption of OTS on the pure silver surfaces (Ag10), (Ag15) and (Ag18)," *University of Thi-Qar Journal of Science*, vol. 10, no. 2, pp. 151-159, 2023.

[30] E. Piosik and M. J. Szary, "Development of MoS2 doping strategy for ehanced SO2 detection at room temperature," 2023.

[31] W. Hou, H. Mi, R. Peng, S. Peng, W. Zeng, and Q. Zhou, "First-principle insight into Ga-doped MoS2 for sensing SO2, SOF2 and SO2F2," *Nanomaterials*, vol. 11, no. 2, p. 314, 2021.

[32] D.-W. Wang *et al.*, "MoTe 2: A promising candidate for SF 6 decomposition gas sensors with high sensitivity and selectivity," *Ieee Electron Device Letters*, vol. 39, no. 2, pp. 292-295, 2017.

[33] H. Cui, H. Zhu, and P. Jia, "Adsorption and sensing of SO2 and SOF2 molecule by Pt-doped HfSe2 monolayer: A first-principles study," *Applied Surface Science*, vol. 530, p. 147242, 2020.

[34] H. Cui, P. Jia, and X. Peng, "Adsorption of SO2 and NO2 molecule on intrinsic and Pd-doped HfSe2 monolayer: A first-principles study," *Applied Surface Science*, vol. 513, p. 145863, 2020.

[35] X. Wang and Y. Liao, "Selective detection of SO 2 in SF 6 insulation devices by Rh-doped HfSe 2 monolayer: A first-principles study," *Applied Physics A*, vol. 125, pp. 1-8, 2019.

[36] N. H. Ali and L. F. Al-Badry, "Enhancing Adsorption and Sensing Performances of Pristine and Ni Cluster Doped HfSe2 Monolayers to SF6 Decomposition Gases: A DFT Study," *Computational and Theoretical Chemistry*, vol. 1226, p. 114207, 2023.

[37] D.-H. Baek and J. Kim, "MoS2 gas sensor functionalized by Pd for the detection of hydrogen," *Sensors and Actuators B: Chemical*, vol. 250, pp. 686-691, 2017.

[38] F. Xiao, W. Lei, W. Wang, L. Xu, S. Zhang, and X. Ming, "Pentagonal two-dimensional noble-metal dichalcogenide PdSSe for photocatalytic water splitting with pronounced optical absorption and ultrahigh anisotropic carrier mobility," *Journal of Materials Chemistry C*, vol. 9, no. 24, pp. 7753-7764, 2021.

[39] W. Lei *et al.*, "A new 2D high-pressure phase of PdSe 2 with high-mobility transport anisotropy for photovoltaic applications," *Journal of Materials Chemistry C*, vol. 7, no. 7, pp. 2096-2105, 2019.

[40] H. Wu, Y. Xia, C. Zhang, S. Xie, S. Wu, and H. Cui, "Adsorptions of C5F10O decomposed compounds on the Cu-decorated NiS2 monolayer:

a first-principles theory," *Molecular Physics*, vol. 121, no. 3, p. e2163715, 2023.
[41] Y. Ma, X. Gong, F. Xiao, Y. Liu, and X. Ming, "First-Principles Calculations of Two-Dimensional Monolayer PdSe2 for Selective Sensing of Nitrogen-Containing Gases," *ACS Applied Nano Materials*, vol. 5, no. 8, pp. 11519-11528, 2022.
[42] S. Zhai *et al.*, "Single Rh atom decorated pristine and S-defected PdS2 monolayer for sensing thermal runaway gases in a lithium-ion battery: A first-principles study," *Surfaces and Interfaces*, vol. 37, p. 102735, 2023.
[43] P. Ou, P. Song, X. Liu, and J. Song, "Superior sensing properties of black phosphorus as gas sensors: a case study on the volatile organic compounds," *Advanced Theory and Simulations*, vol. 2, no. 1, p. 1800103, 2019.
[44] W. Lei *et al.*, "Ferroelastic lattice rotation and band-gap engineering in quasi 2D layered-structure PdSe 2 under uniaxial stress," *Nanoscale*, vol. 11, no. 25, pp. 12317-12325, 2019.
[45] D. M. Guzman and A. Strachan, "Role of strain on electronic and mechanical response of semiconducting transition-metal dichalcogenide monolayers: An ab-initio study," *Journal of Applied Physics*, vol. 115, no. 24, 2014.
[46] D. Li *et al.*, "First-principle insight into the Ru-doped PtSe2 monolayer for detection of H2 and C2H2 in transformer oil," *ACS omega*, vol. 5, no. 49, pp. 31872-31879, 2020.
[47] R. Zhao *et al.*, "External electric field and strains facilitated nitrogen dioxide gas sensing properties on 2D monolayer and bilayer SnS2 nanosheets," *Applied Surface Science*, vol. 491, pp. 128-137, 2019.
[48] J. Ni, W. Wang, M. Quintana, F. Jia, and S. Song, "Adsorption of small gas molecules on strained monolayer WSe2 doped with Pd, Ag, Au, and Pt: A computational investigation," *Applied Surface Science*, vol. 514, p. 145911, 2020.
[49] B. Delley, "From molecules to solids with the DMol 3 approach," *The Journal of chemical physics*, vol. 113, no. 18, pp. 7756-7764, 2000.
[50] B. Zhu *et al.*, "Monolayer Janus Te 2 Se-based gas sensor to detect SO 2 and NO x: a first-principles study," *Physical Chemistry Chemical Physics*, vol. 23, no. 2, pp. 1675-1683, 2021.
[51] J. P. Perdew, K. Burke, and M. Ernzerhof, "Generalized gradient approximation made simple," *Physical review letters*, vol. 77, no. 18, p. 3865, 1996.
[52] P. Ziesche, S. Kurth, and J. P. Perdew, "Density functionals from LDA to GGA," *Computational materials science*, vol. 11, no. 2, pp. 122-127, 1998.
[53] A. Tkatchenko and M. Scheffler, "Accurate molecular van der Waals interactions from ground-state electron density and free-atom reference data," *Physical review letters*, vol. 102, no. 7, p. 073005, 2009.
[54] N. H. Ali and L. F. Al-Badry, "Improvement of sensing performance of SO2, SOF2, and SO2F2 gases on monolayer and bilayer HfSe2 under electric field," *Micro and Nanostructures*, vol. 182, p. 207654, 2023.
[55] H. Wu, B. Zhang, X. Li, and X. Hu, "First-principles screening upon Pd-doped HfSe2 monolayer as an outstanding gas sensor for DGA in transformers," *Computational and Theoretical Chemistry*, vol. 1208, p. 113553, 2022.
[56] H. Yang *et al.*, "Strain-engineered S-HfSe2 monolayer as a promising gas sensor for detecting NH3: A first-principles study," *Surfaces and Interfaces*, vol. 34, p. 102317, 2022.
[57] J. Cao *et al.*, "Controllable gas sensitive performance of 1T'WS2 monolayer instructed by strain: First-principles simulations," *Chemical Physics Letters*, vol. 758, p. 137921, 2020.
[58] Z. Xu, "Ni-Decorated PtS2 Monolayer as a Strain-Modulated and Outstanding Sensor upon Dissolved Gases in Transformer Oil: A First-Principles Study," *ACS omega*, vol. 8, no. 6, pp. 6090-6098, 2023.
[59] V. Kumar, A. Bano, K. Rajput, and D. R. Roy, "The interaction of two-dimensional P2SiS nanosheet with environmental toxic NCG molecules for sensor application: A DFT study," *Sensors and Actuators A: Physical*, vol. 322, p. 112608, 2021.